Original article

Peanut shell from agricultural wastes as a sustainable filler for polyamide biocomposites fabrication

Oumayma Oulidi [a], Asmae Nakkabi [a], Fatima Boukhlifi [b,*], Mohamed Fahim [a], Hassane Lgaz [c], Awad A. Alrashdi [d,*], Noureddine Elmoualij [a]

[a] Laboratory of Bio-inorganic Chemistry, Molecular Materials and Environment, Moulay Ismail University, BP 11201, 50070 Meknes, Morocco
[b] Laboratory of Chemistry and Biology Applied to the Environment, URL-CNRST-N°13, Moulay Ismail University, BP 11201, 50070 Meknes, Morocco
[c] Innovative Durable Building and Infrastructure Research Center, Center for Creative Convergence Education, Hanyang University ERICA,
55 Hanyangdaehak-ro, Sangrok-gu, Ansan-si, Gyeonggi-do, 15588, Korea
[d] Chemistry Department, Umm Al-Qura University, Al-Qunfudah University College, Saudi Arabia

A B S T R A C T

Objective: Natural fibers reinforcements have gained increasing attention for the development of biocomposites thanks to their biodegradability and renewability. The search for natural-based reinforcements that improve the biodegradation of plastics while maintaining their physicochemical and mechanical properties is a never-ending task. Herein, we report the preparation of new biocomposites based on polyamide 6 (PA6) matrix and peanut shell powder (PSP) reinforcement.
Methodology: The biobased composites were prepared by incorporating different amounts of PSP, from 5% to 20% by weight, and then characterized using Fourier transform infrared spectroscopy (FTIR), X-ray diffraction technique (XRD), differential scanning calorimetry (DSC), thermal gravimetric analysis (TGA), and scanning electron microscope (MEB).
Results: Results showed that the addition of PSP did not affect the density of PA6. Its crystallinity was unaffected by the addition of 5%, 10%, and 15% of PSP, while it slightly decreases after the addition of 20% PSP. All analyses showed that the matrix kept its structure after adding a PSP concentration up to 15%, while a higher amount resulted in a new structure.
Conclusion: Results of the present work might open a new way towards the development of efficient biocomposites through the valorization of natural fibers.
© 2022 The Author(s). Published by Elsevier B.V. on behalf of King Saud University. This is an open access article under the CC BY-NC-ND license (http://creativecommons.org/licenses/by-nc-nd/4.0/).

1. Introduction

Polyamides are characterized by their excellent properties, such as outstanding chemical resistance, superior mechanical and thermal properties, good electrical insulation, ease of processing, and coloring. Thanks to these facts, PAs appear ideal for various applications, from furniture, sports, automotive, and textile to fishing industries and the medical sector (Lods et al., 2021; Ogunsona et al., 2017).

PA6 is one of the most used petroleum-based polyamides thanks to its excellent mechanical properties (Young's modulus > 1 GPa) and good thermal resistance (the melting point between 180 and 230 °C), to reference a few (Hafsaoui, 2014). Its annual global production and PA6,6 count for about 95% of PAs (Oelmann and Meier, 2015; Tieke, 2014). Many of these materials are polyamide blends and fossil-based polyamides with a variety of moieties. Meanwhile, in recent years, there has been an increasing demand for PA derivatives from renewable resources due to economic and ecological issues such as emission of greenhouse gasses, the rise of petrochemicals prices, and limited fossil fuel reserves (Spierling et al., 2018). All existing materials exhibit outstanding properties; however, most of the used fillers and reinforcement, such as glass and carbon, are non-renewable materials ("A critical

* Corresponding authors at: Laboratory of Chemistry and Biology Applied to the Environment, URL-CNRST-N°13, Moulay Ismail University, BP 11201, 50070 Meknes, Morocco (F. Boukhlifi).

E-mail addresses: f.boukhlifi@umi.ac.ma (F. Boukhlifi), aarashdi@uqu.edu.sa (A. A. Alrashdi).

Peer review under responsibility of King Saud University.

review on the fabrication processes and performance of polyamide biocomposites from a biofiller perspective," 2019; Brehmer, 2013; Spierling et al., 2018). With the growing interest in green chemistry, preparing PAs materials using biobased materials is no longer a choice but a requirement to balance the economy and environment and ensure the development of durable materials (Alashwal et al., 2020; Chen et al., 2020).

More recently, scientific and industrial communities have shown a keen interest in exploiting natural fibers from agricultural resources as a reinforcing additive in polymer biocomposites (Puglia et al., 2005; Rao and Rao, 2007). Natural fibers can be used as substitute fillers for clay, carbon, glass, and aramid fibers, avoiding toxic by-products during manufacturing processes (Satyanarayana et al., 2009). This interest is driven by the low cost, availability, good resistance properties, low density, and excellent biodegradability of these biobased materials (Aminullah et al., 2010; Baiardo et al., 2004; Elanchezhian et al., 2018; Lau et al., 2018). By incorporating these fillers into synthetic polymers, new biocomposite materials can be developed for different applications such as construction and automotive industries, packaging and furniture, etc. (Codou et al., 2018; Lods et al., 2021; Oelmann and Meier, 2015; Ogunsona et al., 2017; Revol et al., 2021).

Many animal and lignocellulosic materials have been used as biobased fillers with properties that compete well with their synthetic counterparts (Aminullah et al., 2010; Baiardo et al., 2004; Lau et al., 2018). Peanut shell powder (PSP) is a lignocellulosic material composed of cellulose, hemicelluloses, and lignin. Like most agricultural residues, peanut shells are produced in large quantities every year and discharged into the environment without proper treatment or used as animal feeds in the best-case scenario. Hence, its use as a biobased filler is worth exploring. Recently, the PSP has been successfully used as a reinforcing filler in urea–formaldehyde resin (Guler and Büyüksarı, 2011) and epoxy resin (Raju and Kumarappa, 2011). Nutshells from walnut, almond, and pistachio have been used as fillers in low-density polyethylene (LDPE) and polylactic acid (PLA) polymers (Sutivisedsak et al., 2012). The authors reported a slight influence of fillers on the thermal properties while the mechanical properties showed a slight decrease. Muralidhar et al.(Muralidhar et al., 2020) applied a 15 wt% of a treated areca nut husk fiber as filler in an epoxy. The resulted composite showed improved elastic properties. In another research effort, bagasse waste was used as a reinforcing filler to prepare wooden/polymer composites by Naguib et al.(Naguib et al., 2015). The authors used unsaturated polyester resin with 5, 10, and 15% of treated and untreated bagasse; they reported an improved flexural strength by incorporating alkali-treated bagasse and a reduced flexural strength by untreated bagasse. These works and many others highlight the significant importance of employing agricultural wastes as reinforcing fillers to prepare biocomposite materials. A recent review by E. Kuram reported the recent progress in using natural fibers to prepare biocomposites (Kuram, 2021).

Considering the above, this work intends to contribute to this area by developing new biocomposite materials based on PA6 and PSP. The preparation of PA6 was carried out by anionic polymerization via ring-opening of the ε-caprolactam (ε-CL) monomer using an initiator and an activator. Then, the incorporation of the natural PSP is carried out by in-situ polymerization. The prepared biocomposite was characterized using fourier transform infrared spectroscopy (FTIR), X-ray diffraction technique (XRD), differential scanning calorimetry (DSC), and thermal gravimetric analysis (TGA). Its morphology was also studied using a scanning electron microscope (MEB). The new biocomposites reported in this work could be of particular interest for further exploitation and application.

2. Materials and methods

2.1. Synthesis of PA6

All chemicals and reagents used in this work, including ε-Caprolactam, N-acetylcaprolactam, and NaOH were purchased from Sigma-Aldrich and used without further treatment. The polymerization was carried out in two oil baths, one held at 80 °C and the other at 130 °C. A 2.5 g of ε-Caprolactam was introduced into each of the two test tubes and brought to fusion at 80 °C for 5 to 10 min. Then, a 0.15 g of NaOH as initiator was carefully placed in one of the tubes with the molten ε-Caprolactam. The test tube was gently shaken to homogenize the mixture, where a spontaneous reaction took place, as indicated by hydrogen evolution. A 0.320 mL of N-acetylcaprolactam was introduced into the other test tube using an Eppendorf pipette and maintained for ∼ 10 min at 80 °C, then at 130 °C for 10 min. The molten activator was then poured into the test tube with the molten mass of the initiator, and the mixture was homogenized by brief stirring. The polymer was kept at 130 °C for 20 min, then cooled and removed by breaking the test tube and finally ground.

2.2. Preparation of PA6/PSP biocomposites

The same protocol used for the synthesis of PA6 was followed here, except the quantity of ε-Caprolactam was subtracted and replaced by the reinforcement according to the following ratios: 2%, 10%, 15%, and 20% in weight. These quantities were added to the test tube containing the molten mass of the initiator and subjected to agitation at 100 rpm for 5 to 10 min to ensure the homogenization of the medium and the dispersion of the reinforcement within the matrix. The molten activator was then poured into the test tube with the molten mass of the initiator, and the mixture was homogenized by brief stirring. The mixture is maintained at 130 °C for 20 min and then at 140 °C for 10 min. The obtained biocomposite was cooled in the open air, then removed by breaking the test tube, and finally ground.

2.3. Characterization techniques

The nature of chemical bonds and functional groups of PA, PSP (Fig. 1), and biocomposite materials was investigated using Fourier Transform Spectrophotometer (Jasco FT/IR-4100, Tokyo, Japan) in 4000–400 cm^{-1} infrared spectrum range. The structural analysis by X-ray diffraction (DRX) was carried out on a diffractometer type X-RD-6100-Shimadzu (XRD-6100, Shimadzu, Japan) with λ_{Cu} = 1.54 Å. The diffraction spectrum was obtained at 2 ⊖ values between 2 and 80°, at a scanning speed of 1°/ min. Differential scanning calorimetry (Setaram DSC 131 Evo) was used for calorimetric measurements. The heating rate was fixed at 10 °C / min, under a 20 mL/ min of nitrogen flow rate. The device operates between −170 °C and 700 °C. A Shimadzu TG-60 equipment was used for thermogravimetric measurements. It operates between room temperature and 900 °C, with freely adjustable heating rates between 0.001 and 100 °C/ min. The morphology of the prepared material was examined by a JEOL JSM-IT 500 HR scanning electron microscope operating at a 5 kV accelerating voltage and under secondary electron image mode.

3. Results and discussions

3.1. FT-IR analysis

The FTIR spectra of PA6 are represented in Figure S1(a) (supplementary material). The strong absorption bands positioned at
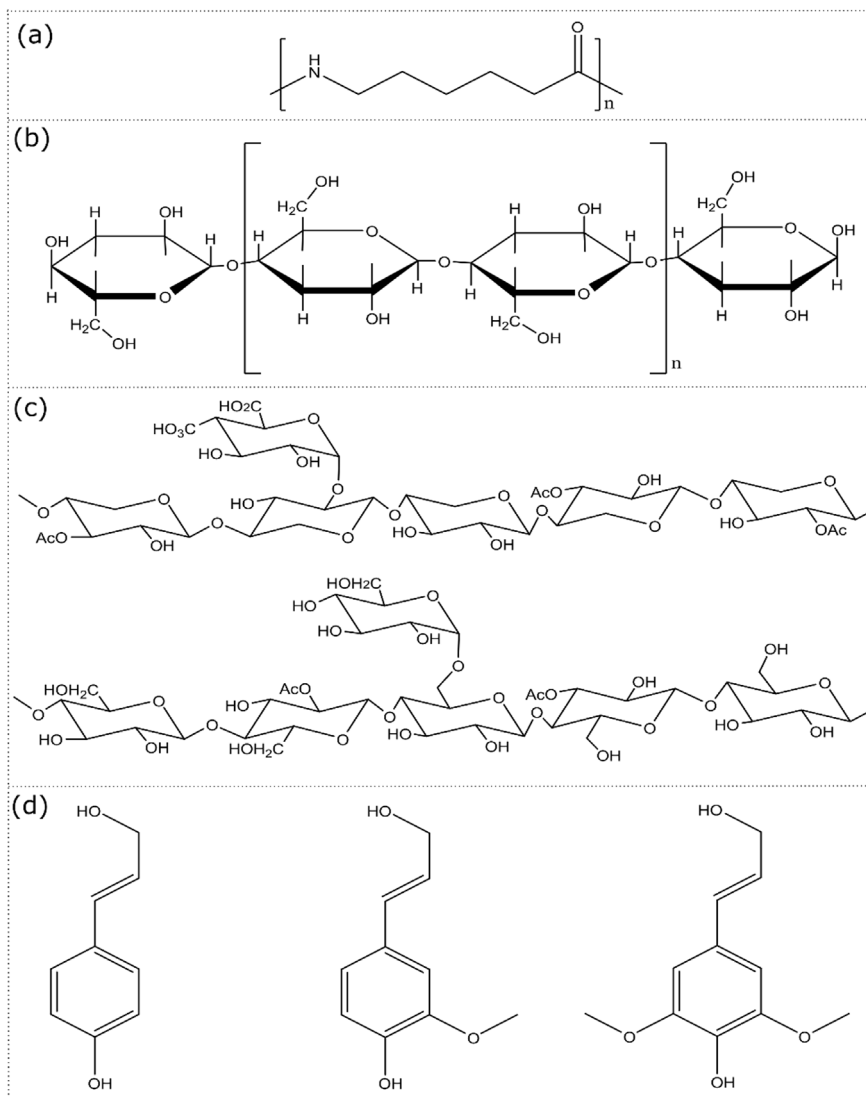
Fig. 1. Molecular structure of (a) polyamide 6, and (b)-(d) PSP's main components. (b) Cellulose, (c) hemicellulose, and (d) main components of lignin.

3350–3250 cm^{-1} and 1560–1530 cm^{-1} are attributed to the elongation and the deformation of the NH, respectively. The bands located at 2940–2910 cm^{-1} and 2870–2840 cm^{-1} can be assigned to the deformation of the group (CH$_2$)5. The strong band around 1660–1630 cm^{-1} is associated with elongation of the carbonyl group C = O. The weak bands positioned at 3105–3075 cm^{-1}, 1270–1240 cm$^{-1,}$ and 740–650 cm^{-1} can be due to NH deformation, while that at 1270–1240 cm^{-1} can be attributed to a CN elongation (Vasanthan and Salem, 2001).

The functional groups of the PSP were also investigated using FT-IR, as shown in Figure S1(b). The absorption bands located at 3434 cm^{-1} are attributed to OH of the cellulose group or the phenol group of lignin [21]. At 2919 cm^{-1} corresponds to the CH group of methyl or methylene group. The methoxy group of hemicellulose and lignin can be identified from the band at 2851 cm^{-1} (Ikladious et al., 2017). In addition, the band at 1637 cm^{-1} is attributed to the carbonyl group C = O of the acetyl group of lignin and hemicellulose (Punnadiyil et al., 2016).

Furthermore, the effect of thermal conditions during polymerization on the chemical structure of PSP was studied using FT-IR. The PSP was subjected to a temperature ranging from 130 °C to 140 °C for 30 min. Results are shown in Figure S1(c), when one can observe a displacement of the band at 1002 cm^{-1} towards the very intense band 1029 cm^{-1}, which can be attributed to CH of glucose or to CO–(H) of the phenol group of the xylan group (hemicelluloses) (Zhang et al., 2019). In addition, results reveal the appearance of a peak at 1732 cm^{-1} due to dehydration and the formation of the C = O group of lignin and hemicelluloses (Ikladious et al., 2017).

FTIR analysis was also performed to identify the functional groups of the prepared biocomposites and potential interactions between filler and PA6. The FTIR spectra of the PSP and the biocomposites are shown in Fig. 2. Results indicate that all the IR spectra of the biocomposites (2%, 10%, 15%, and 20%) have the same characteristic bands as the raw PA6. From Fig. 2, one remark that bands located at 1029 cm^{-1} and 1732 cm^{-1} disappear. This can be explained by the interaction between the hydroxyl group (C-OH) and the ester group of the cellulose, giving rise to new hydrogen bonds, as shown in Fig. 3. The same results were obtained by Zaaba et al. in their study on the effect of peanut shell powder on the properties of recycled polypropylene (Zaaba et al., 2013).
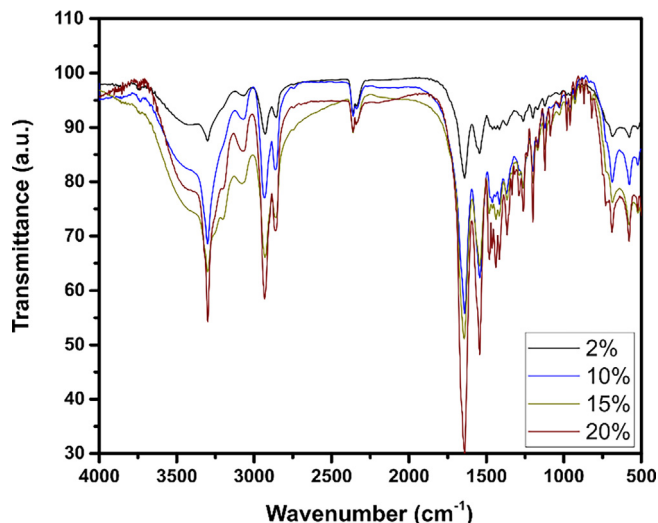
Fig. 2. FTIR spectra of PA6/PSP biocomposites.

3.2. Effect of PSP on PA density

The effect of incorporating PSP into the PA6 matrix on its density was studied by determining the density of the prepared biocomposites. From Fig. 4, we can conclude that the PA6 density is 1.14 g/cm³ at 20 °C, which agrees with previously reported results (Filippone et al., 2010; Hamid et al., 2013; Iqbal et al., 2010; Liu et al., 2014). It can be concluded that the addition of PSP into the PA6 matrix is not accompanied by any change in density when the PSP content increases. This indicates that biocomposites with interesting properties could be prepared (Baiardo et al., 2004).

3.3. XRD analysis

The crystal structure of different materials was analyzed by X-ray diffraction technique. The diffractogram and its deconvolution represented in Figures S2(a)-(b) indicate that PA6 shows two distinguished reflections at $2\ominus =19.94$ and $23.88°$ corresponding crystal planes $(1\,0\,0)$ (Kuo et al., 2006) and $(0\,0\,2/2\,0\,2)$ (Dencheva et al., 2014), respectively. These reflections are assigned to the thermodynamically stable crystalline phase α-monoclinic. In addition, the metastable γ phase of PA6 can be observed at $2\ominus = 19.81°$ after a deconvolution (Figure S2(b)) (Lecocq, 2012).

The crystallinity of the reinforcement was studied using an X-ray diffractogram to predict its impact on the crystallinity of the biocomposite. From the results in Figure S2(c), two peaks can be observed at the maximum diffraction positions $2\theta = 15°$ and $2\theta = 21.86°$, corresponding to the crystallographic plane 002. This indicates the crystalline regions of cellulose characteristic of ligno-cellulosic materials (SANTOS, 2018), which agrees with a previous study (Ikladious et al., 2017).

The addition of 2%, 10%, and up to 15% has no impact on the crystal structure of the prepared biocomposite. In contrast, the addition of 20% results in six additional diffraction peaks, as shown in Fig. 5. An average diffraction peak at $2\ominus = 16.91°$, four weak peaks towards $2\ominus = 9.76°$, $2\ominus = 14°$, $2\ominus = 22°$ and $2\ominus = 23°$ and a strong peak at $2\ominus = 18.21°$. These four weak peaks were a distinguishing characteristic of PSP. The medium and strong peaks are both caused by the intercalation of PSP in the chains of the PA6 macromolecule, which means that the d_{hkl} between the plane $(1\,0\,0)$ is reduced as the structure of PA6 is modified by adding PSP, weakening; therefore, the hydrogen bond within the PA6 matrix (Cristina et al., 2012).

The presence of the peanut shell does not significantly change the crystallinity rate %Xc. The results in Table 1 show that the crystallinity rate is between 35 and 39%, which implies that the PA6
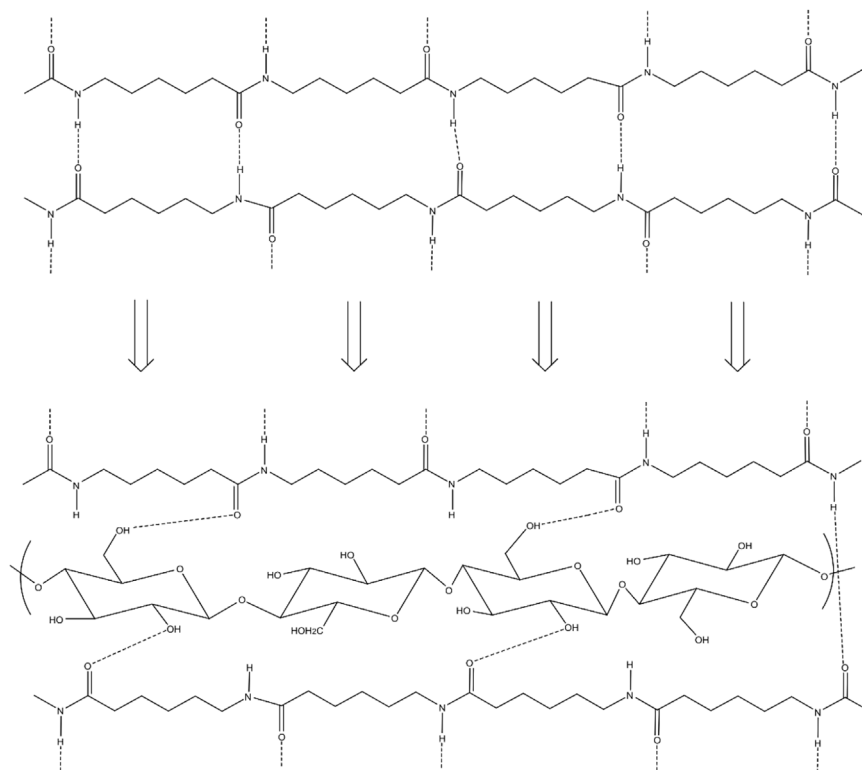

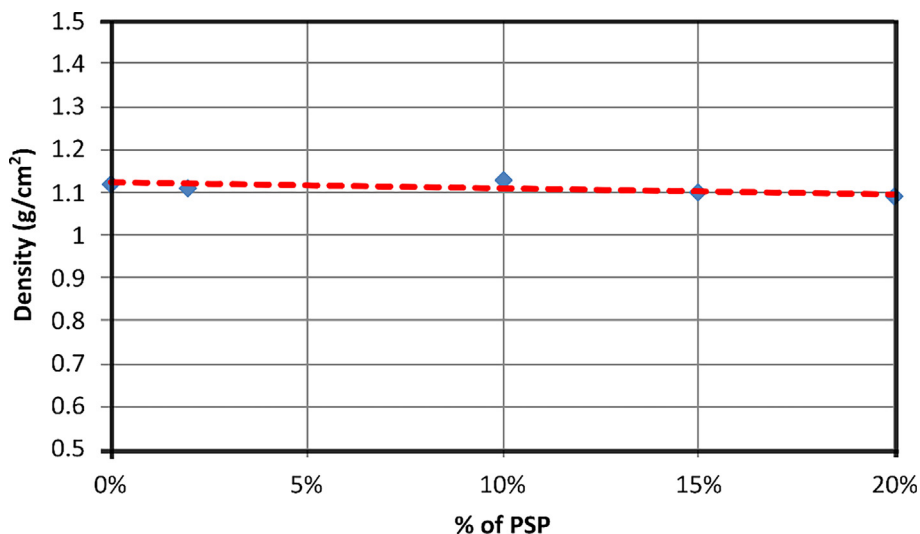**Fig. 3.** Formation of hydrogen bonds within the biocomposites.

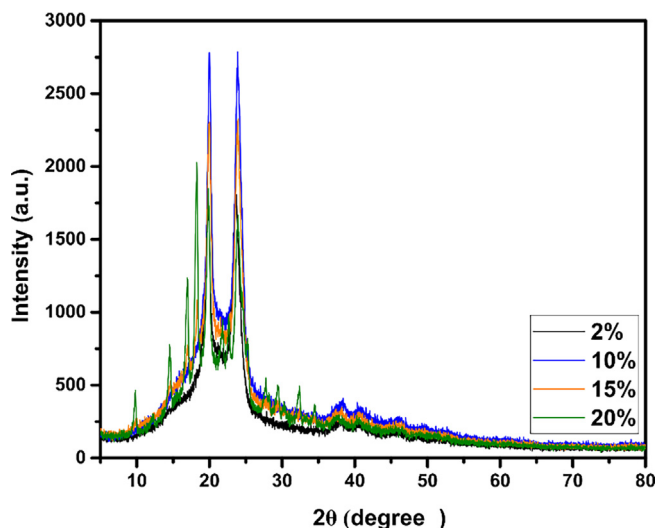Fig. 4. Density of PA6 and PA6/PSP biocomposites.

Fig. 5. X-ray diffraction patterns of PA6/PSP biocomposites.

matrix and the PSP keep most of their crystalline zones and that the macromolecular chains attach to the main components of PSP, namely cellulose, by creating other crystalline zones that overlap with those already existing within the PA6 and PSP matrix. This ensures a balanced crystallinity within the biocomposite.

3.4. Thermal properties

The differential scanning calorimetry was used to study the thermal properties of PA6. The DSC thermogram in Fig. 6(a) shows a double endothermic peak of fusion during the heating sweep T_{m1} = 199 °C and T_{m2} = 203 °C attributed to the α and γ crystalline phases of PA6. A previous study has already reported this behavior (Alvarez and Valle, 2012). PA6 is well known for its strong hydrogen bonding capacity (H-bond), which dominates the physical

behavior of PA6 (Ahmadi et al., 2010). The effect of PSP incorporation on the crystallization behavior and fusion of PA6 was evaluated by DSC as shown in Fig. 6(b). The glass transition (T_g) and the melting temperature (T_m) are listed in Table 2. It can be seen from Table 2 that the addition of PSP does not significantly alter the Tg of the biocomposites. Most of the first scans of the prepared biocomposites show only one melting peak ranging between 171 and 204 °C, suggesting that the crystal structure of the biocomposites essentially consists of thermodynamically stable α type crystals (Dencheva et al., 2014). The disappearance of the double peak is mainly due to the reorganization of the crystalline zones within the biocomposite.

The addition of PSP in PA6 at an increased concentration of 2%, 10%, and 15% results in a modification of the thermal behavior of PA6. The endothermic peak is shifted to a lower temperature 201 to 198 °C. The higher the PSP concentration, the greater the endothermic peak, probably due to an increased concentration of nucleation centers generating smaller crystallites (Panaitescu et al., 2007). On the other hand, the T_m of the biocomposite decreases when the content of 20% by weight of PSP is incorporated into the PA6 matrix. This decrease can be due to more than one reason. One of the reasons is that the macromolecules might become more spaced apart. It can also be due to a slight minimization of the hydrogen bonds within the PA6 macromolecule, which decreases the crystal size and content, thereby decreasing the melting temperature (Panaitescu et al., 2007). The thermal properties of the biocomposites remain attractive to up to 15% of the PSP. Despite the slight decrease in the T_m after the addition of 20% by weight of PSP, the biocomposites still could be excellent candidates for practical use in different applications.

3.5. Thermo-gravimetric analysis

The thermal degradation of PA6 was studied by thermogravimetric analysis in an air atmosphere up to 600 °C at a heating rate of 10 °C/min. Fig. 7(a) shows that the initial degradation temperature is around 180 °C with a very low mass loss of 6%, possibly

Table 1
Crystallinity rate of the biocomposites determined by XRD.

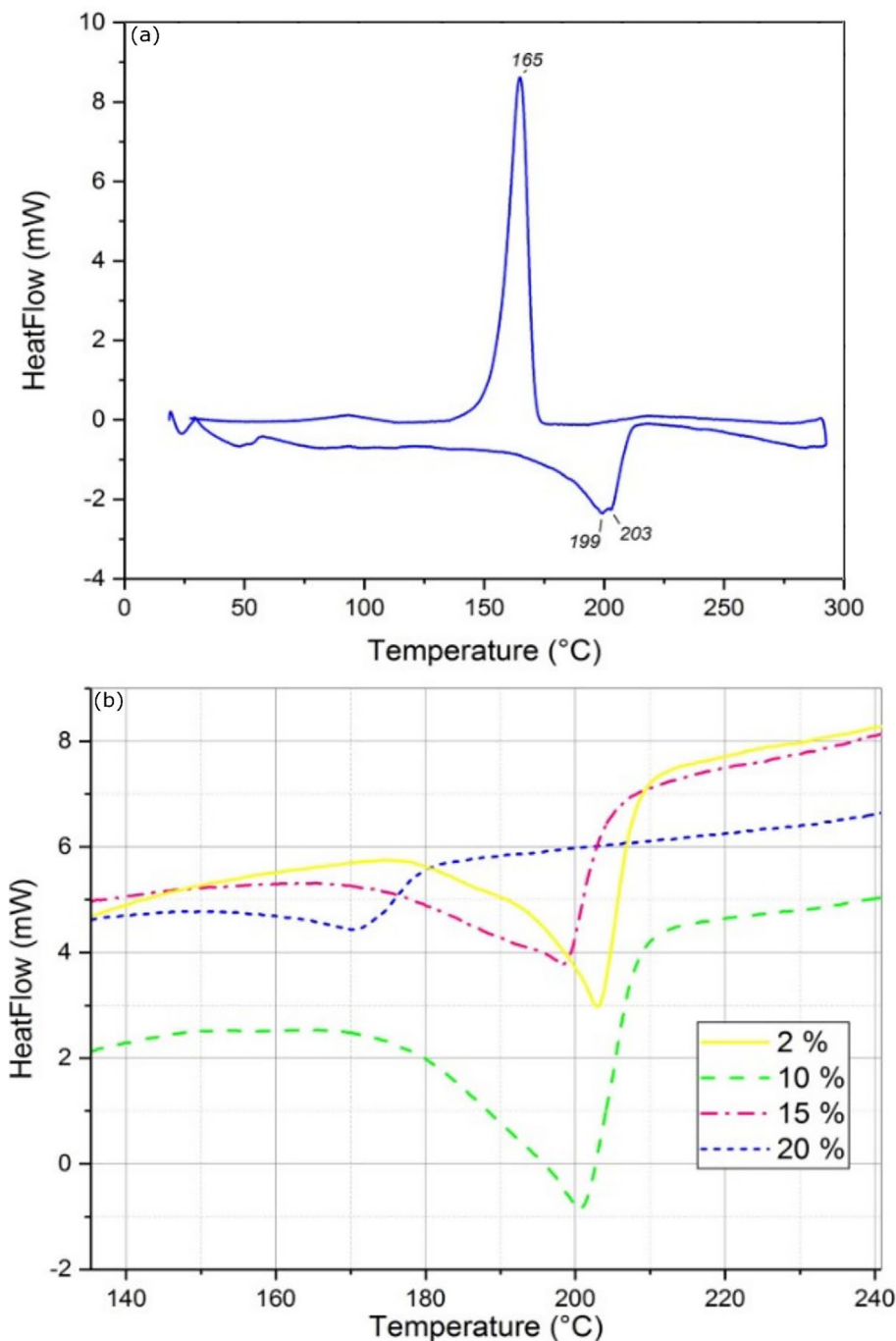| PSP (% in weight)	0	2	10	15	20	100
Xc (%)	39	38	38	35	35	35

Fig. 6. DSC thermograms of (a) PA6, and (b) PA6/PSP biocomposites.

resulting from traces of reactive system residues. When the temperature increases up to 380 °C, a very significant mass loss exceeding 80% can be observed, mainly due to the cleavage of

Table 2
Thermal properties collected from the DSC thermogram of PA6/PSP biocomposites.

% of PSP	T_g (°C)	T_m (°C)
0	38	204
2	32	203
10	32	201
15	32	198
20	30	171

the C–C bond leading to depolymerization. This phenomenon has also been reported in previous investigations (Mark et al., 1975).

TG analysis was performed for peanut shells under the same conditions to get some insights into their thermal behavior. As can be seen in Figure S3, there are three stages of weight loss. The first region is at 130–170 °C, the second at 250–400 °C, and a third one is above 450 °C. At around 160 °C, the mass loss is due to the loss of bound-water molecules and other volatile substances present in the peanut shell (Zierdt et al., 2015). The decomposition temperature at 250 to 400 °C indicates the thermal degradation of hemicellulose and cellulose, while that above 400 °C is attributed to the carbonization process of lignin. These results match well with those reported by several authors (Fernandes et al., 2017; Monteiro et al., 2012; Shang et al., 2015).
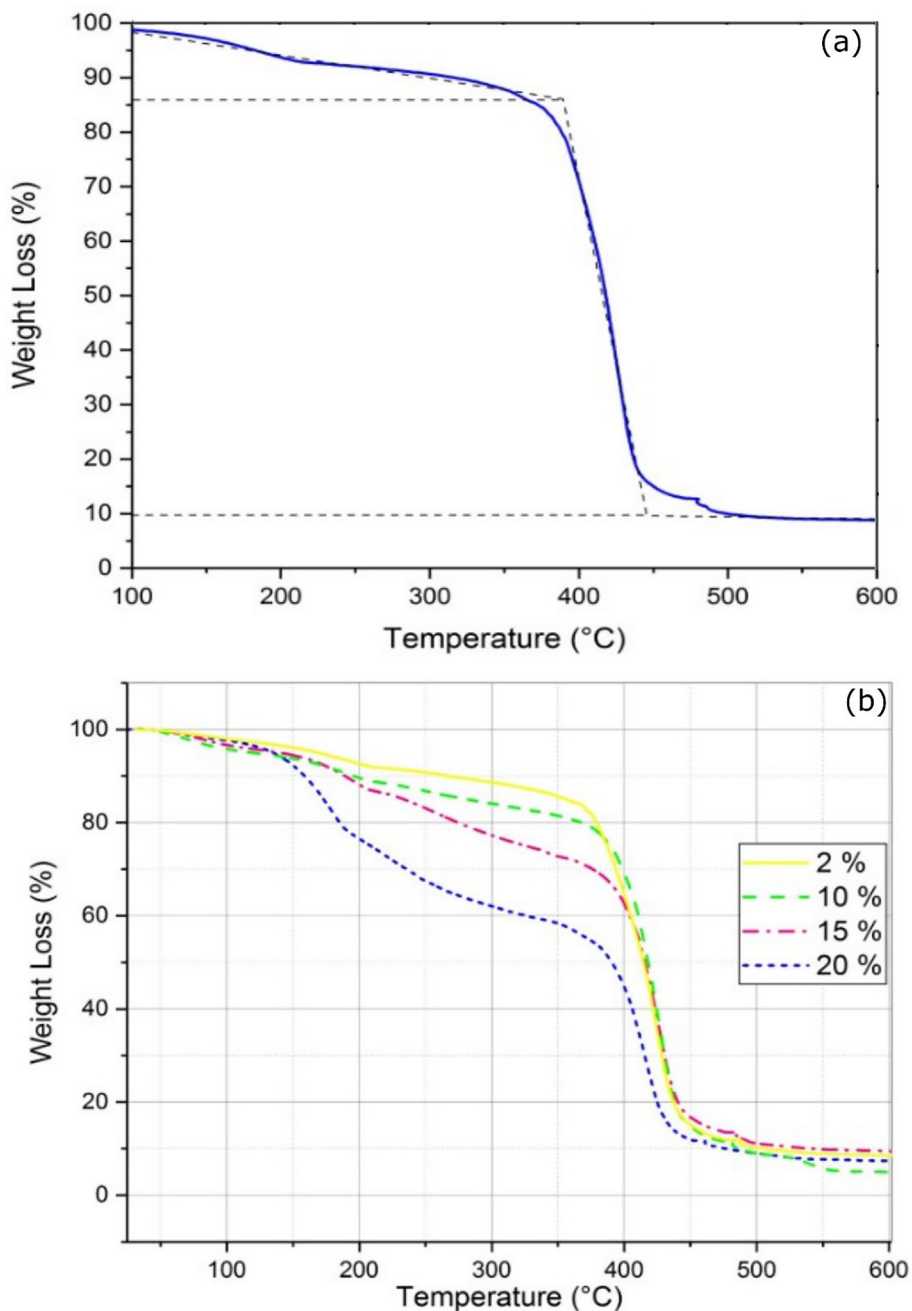
Fig. 7. TGA curves of (a) PA6, and (b) PA6/PSP biocomposites.

On the other hand, the effect of PSP addition on the thermal properties of biocomposites was also investigated using TGA. Interestingly, the thermograms for biocomposites containing 2% and 10% show mass losses similar to PA6. In contrast, incorporating 15% and 20% by weight of the PSP within the macromolecule PA6 affects the thermal decompositions. Results in Fig. 7(b) show a mass loss of 10% and 20% for 15% and 20%, respectively, at 147–350 °C. This can be due to a successive loss of small PSP and PA6. In addition, a mass loss of 65% and 50% is recorded for 15% and 20%, respectively, at 370–450 °C. These mass losses could be due to the chain splitting process, the rupture of carbon–carbon bond occurring, particularly at the level of the PA6 matrix, and/or the breakage of the hydrogen bonds formed between the macromolecule PA6 and the PSP.

3.6. SEM analysis

SEM analysis was performed to visualize PSP dispersion in the PA6 matrix. The SEM images of PA6, PSP, and biocomposites with 10% and 20% of PSP are illustrated in Fig. 8. The SEM image of PA shown in Fig. 8a shows a semi-crystalline morphology with a multitude of crystals of cubic shape and others in the form of a needle or stick dispersed over the entire surface. In the case of PSP, the SEM image in Fig. 8b shows a morphology with stiff, compact, disorganized, and tangled rod or rod-shaped fibers. However, after incorporating PSP, the semi-crystalline character is changed to the distribution of dispersed particles. Empty pores of irregular shapes and different sizes are randomly distributed throughout the surface, as shown in Fig. 8c. This effect can be clearly noticed
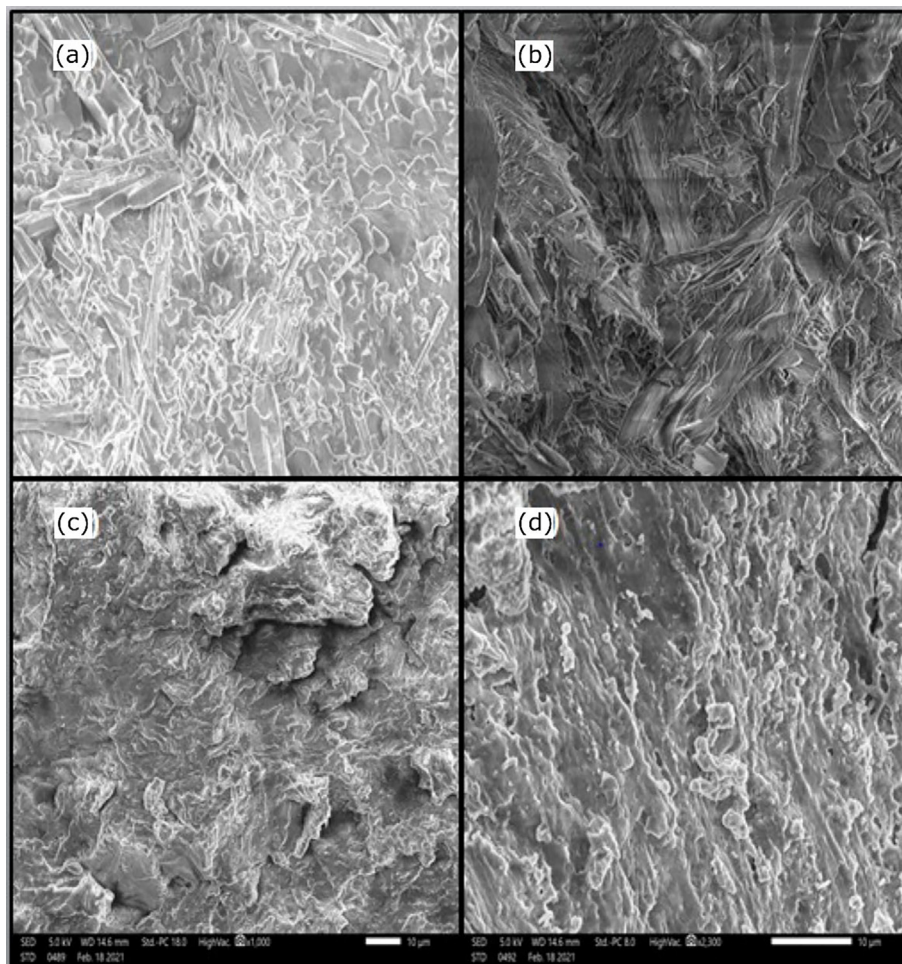
Fig. 8. SEM micrographs of (a) PA6, (b) PSP, (c) PSP(10%)/PA6, (d) PSP(20%)/PA6.

when increasing the amount of incorporated PSP in the PA6 matrix (Fig. 8d). These observations confirm favorable interactions between PA6 and PSP, as already mentioned in the structural characterization of obtained biocomposites.

4. Conclusions

The present work reported preparing new biocomposites through in-situ polymerization of peanut shell in PA6 by anionic activation of ε-CL to improve its biodegradability. Biocomposites were synthesized with different amounts of PSP (5% to 20%) and characterized using various characterization techniques. The density of biocomposites was found to be close to that of PA6. The FTIR analysis showed that the reinforced biocomposites exhibited good reinforcement/matrix interactions. DRX studies of the three constituents, PA6, PSP, and biocomposites, showed a homogeneous distribution of PSP within the PA6 matrix, with almost unchangeable crystallinity. The DSC analysis demonstrated the formation of biocomposites with crystals only in the α phase. The absence of γ phase implied better thermal and structural properties. Among the prepared biocomposites, the addition of 20% PSP affected the thermal properties of PA6. TGA measurements showed a significant change in the decomposition temperature of biocomposites with higher PSP concentrations, while small concentrations, i.e., 2% and 10% of PSP had more negligible effect. The search for natural fibers as green alternatives to inorganic fillers has created great opportunities to develop green composites. Therefore, considering the environmental and ecological concerns, this research direction should be expanded to discover all potential applications of agricultural wastes in the development of biocomposites. The present work is an effort toward this objective, which showed promising results that could open the way for further investigations.

Declaration of Competing Interest

The authors declare that they have no known competing financial interests or personal relationships that could have appeared to influence the work reported in this paper.

Acknowledgements

Appendix A. Supplementary data

Supplementary data to this article can be found online at https://doi.org/10.1016/j.jksus.2022.102148.

References

Ahmadi, S., Morshedian, J., Hashemi, S.A., Carreau, P.J., Leelapornpisit, W., 2010. Novel anionic polymerization of e–caprolactam towards polyamide 6 containing nanofibrils. Iranian Polymer Journal 19, 229–240.

Alashwal, B.Y., Saad Bala, M., Gupta, A., Sharma, S., Mishra, P., 2020. Improved properties of keratin-based bioplastic film blended with microcrystalline cellulose: A comparative analysis. Journal of King Saud University - Science 32, 853–857. https://doi.org/10.1016/j.jksus.2019.03.006.

Alvarez, E.N.C., Valle, L.F.R. De, 2012. Influence of Laurolactam Content on the Clay Intercalation of Polyamide 6 , 12 / Clay Nanocomposites Synthesized by Open Ring 2012. https://doi.org/10.1155/2012/487948.

Aminullah, A., Syed Mustafa, S.J., Nor Azlan, M.R., Mohd. Hafizi, N., Mohd. Ishak, Z.A., Rozman, H.D., 2010. Effect of filler composition and incorporation of additives on the mechanical properties of polypropylene composites with high loading lignocellulosic materials. Journal of Reinforced Plastics and Composites 29 (20), 3115–3124.

Baiardo, M., Zini, E., Scandola, M., 2004. Flax fibre–polyester composites. Composites Part A: Applied Science and Manufacturing 35, 703–710. https://doi.org/10.1016/j.compositesa.2004.02.004.

Brehmer, B., 2013. Polyamides from Biomass Derived Monomers, in: Bio-Based Plastics. John Wiley & Sons, Ltd, pp. 275–293. https://doi.org/10.1002/9781118676646.ch10.

Chen, M., Zhang, H., Shan, S., Li, Y., Li, X., Peng, D., 2020. Fabrication of multiwalled carbon nanotubes/carrageenan-chitosan@ Ce and Sr substituted hydroxyapatite biocomposite coating on titanium: In vivo bone formation evaluations. Journal of King Saud University - Science 32, 1175–1181. https://doi.org/10.1016/j.jksus.2019.11.006.

Codou, A., Misra, M., Mohanty, A.K., 2018. Sustainable biocarbon reinforced nylon 6/polypropylene compatibilized blends: Effect of particle size and morphology on performance of the biocomposites. Composites Part A: Applied Science and Manufacturing 112, 1–10. https://doi.org/10.1016/j.compositesa.2018.05.018.

Cristina, R., Reis, N., Magalhães, F., Mendes, T., Perrone, C.C., Anna, C.S., Souza, W.D., Abud, Y., Pinto, E., Ferreira-leitão, V., 2012. Structural evaluation of sugar cane bagasse steam pretreated in the presence of CO 2 and SO 2. Biotechnology for biofuels 5, 36. https://doi.org/10.1186/1754-6834-5-36.

Dencheva, N., Gaspar, H., Filonovich, S., Lavrova, O., Busani, T., Bernardo, G., Denchev, Z., 2014. Fullerene-modified polyamide 6 by in situ anionic polymerization in the presence of PCBM. Fullerene-modified polyamide 6 by in situ anionic polymerization in the presence of PCBM 49 (14), 4751–4764.

Elanchezhian, C., Ramnath, B.V., Ramakrishnan, G., Rajendrakumar, M., Naveenkumar, V., Saravanakumar, M.K., 2018. Review on mechanical properties of natural fiber composites. Materials Today: Proceedings 5 (1), 1785–1790.

Fernandes, F.C., Gadioli, R., Yassitepe, E., Paoli, M.-A.-D., 2017. Polyamide-6 composites reinforced with cellulose fibers and fabricated by extrusion: Effect of fiber bleaching on mechanical properties and stability. Polymer Composites 38, 299–308. https://doi.org/10.1002/pc.23587.

Filippone, G., Dintcheva, N.T., La Mantia, F.P., Acierno, D., 2010. Using organoclay to promote morphology refinement and co-continuity in high-density polyethylene/polyamide 6 blends – Effect of filler content and polymer matrix composition. Polymer 51, 3956–3965. https://doi.org/10.1016/j.polymer.2010.06.044.

Guler, C., Büyüksarı, Ü., 2011. EFFECT OF PRODUCTION PARAMETERS ON THE PHYSICAL AND MECHANICAL PROPERTIES OF PARTICLEBOARDS MADE FROM PEANUT (Arachis hypogaea L.) HULL. BioResources 6, 5027–5036.

Hafsaoui, S.L., 2014. Etude et modélisation de la stabilité thermique et des propriétés des polyamides au cours du rotomoulage. Ecole nationale supérieure d'arts et métiers - ENSAM.

Hamid, F., Akhbar, S., Halim, K.H.K., 2013. Mechanical and Thermal Properties of Polyamide 6/HDPE-g- MAH/High Density Polyethylene. Procedia Engineering, INTERNATIONAL TRIBOLOGY CONFERENCE MALAYSIA 2013 (68), 418–424. https://doi.org/10.1016/j.proeng.2013.12.201.

Ikladious, N.E., Shukry, N., El-Kalyoubi, S.F., Asaad, J.N., Mansour, S.H., Tawfik, S.Y., Abou-Zeid, R.E., 2017. Eco-friendly composites based on peanut shell powder / unsaturated polyester resin. Proceedings of the Institution of Mechanical Engineers, Part L: Journal of Materials: Design and Applications 233, 955–964. https://doi.org/10.1177/1464420717722377.

Iqbal, M., Chuai, C., Huang, Y., Che, C., 2010. Modification of low-density polyethylene by graft copolymerization with maleic anhydride and blends with polyamide 6. Journal of Applied Polymer Science 116, 1558–1565. https://doi.org/10.1002/app.31439.

Kuo, P.-C., Sahu, D., Yu, H.H., 2006. Properties and biodegradability of chitosan/nylon 11 blending films. Polymer Degradation and Stability 91 (12), 3097–3102.

E. Kuram Advances in development of green composites based on natural fibers: a review. emergent mater 2021 10.1007/s42247-021-00279-2.

Lau, K., Hung, P., Zhu, M.-H., Hui, D., 2018. Properties of natural fibre composites for structural engineering applications. Composites Part B: Engineering 136, 222–233. https://doi.org/10.1016/j.compositesb.2017.10.038.

Lecocq, E., 2012. Caractérisation et mise en œuvre de systèmes réactifs polyamide et polyépoxyde formulés pour le rotomoulage de liners de stockage hyperbare.

Liu, T., Wang, Q., Xie, Y., Lee, S., Wu, Q., 2014. Effects of use of coupling agents on the properties of microfibrillar composite based on high-density polyethylene and polyamide-6. Polym. Bull. 71, 685–703. https://doi.org/10.1007/s00289-013-1086-x.

Mark, H.F., Atlas, S.M., Shalaby, S.W., Pearce, E.M., 1975. Combustion of Polymers and Its Retardation. In: Lewin, M., Atlas, S.M., Pearce, E.M. (Eds.), Flame-Retardant Polymeric Materials. Springer US, Boston, MA, pp. 1–17.

Monteiro, S.N., Calado, V., Rodriguez, R.J.S., Margem, F.M., 2012. Thermogravimetric Stability of Polymer Composites Reinforced with Less Common Lignocellulosic Fibers – an Overview. Journal of Materials Research and Technology 1, 117–126. https://doi.org/10.1016/S2238-7854(12)70021-2.

Muralidhar, N., Vadivuchezhian, K., Arumugam, V., Srinivasula Reddy, I., 2020. Flexural modulus of epoxy composite reinforced with Arecanut husk fibre (AHF): A mechanics approach. Materials Today: Proceedings 27, 2265–2268.

Naguib, H.M., Kandil, U.F., Hashem, A.I., Boghdadi, Y.M., 2015. Effect of fiber loading on the mechanical and physical properties of "green" bagasse–polyester composite. Journal of Radiation Research and Applied Sciences 8, 544–548. https://doi.org/10.1016/j.jrras.2015.06.004.

Oelmann, S., Meier, M.A.R., 2015. Synthesis of Modified Polycaprolactams Obtained from Renewable Resources. Macromolecular Chemistry and Physics 216, 1972–1981. https://doi.org/10.1002/macp.201500257.

Ogunsona, E.O., Misra, M., Mohanty, A.K., 2017. Sustainable biocomposites from biobased polyamide 6,10 and biocarbon from pyrolyzed miscanthus fibers. Journal of Applied Polymer Science 134. https://doi.org/10.1002/app.44221.

Panaitescu, D.M., Donescu, D., Bercu, C., Vuluga, D.M., Iorga, M., Ghiurea, M., 2007. Polymer Composites With Cellulose Microfibrils. Polymer Engineering & Science 47, 1228–1234. https://doi.org/10.1002/pen.

Puglia, D., Biagiotti, J., Kenny, J.M., 2005. A Review on Natural Fibre-Based Composites—Part II. Journal of Natural Fibers 1, 23–65. https://doi.org/10.1300/J395v01n03_03.

Punnadiyil, R.K., Sreejith, M.P., Purushothaman, E., 2016. Isolation of microcrystalline and nano cellulose from peanut shells. Journal of Chemical and Pharmaceutical Sciences 2016-Janua, 12–16.

Raju, G.U., Kumarappa, S., 2011. Experimental study on mechanical properties of groundnut shell particle-reinforced epoxy composites. Journal of Reinforced Plastics and Composites 30, 1029–1037. https://doi.org/10.1177/0731684411410761.

Rao, K.M.M., Rao, K.M., 2007. Extraction and tensile properties of natural fibers: Vakka, date and bamboo. Composite Structures 77, 288–295. https://doi.org/10.1016/j.compstruct.2005.07.023.

Revol, B.P., Vauthier, M., Thomassey, M., Bouquey, M., Ruch, F., Nardin, M., 2021. Design of experience to evaluate the Interfacial compatibility on high tenacity viscose fibers reinforced Polyamide-6 composites. Composites Science and Technology 203,. https://doi.org/10.1016/j.compscitech.2020.108615 108615.

Satyanarayana, K.G., Arizaga, G.G.C., Wypych, F., 2009. Biodegradable composites based on lignocellulosic fibers-An overview. Progress in Polymer Science (Oxford) 34, 982–1021. https://doi.org/10.1016/j.progpolymsci.2008.12.002.

Shang, H., Lu, Y., Zhao, F., Chao, C., Zhang, B., Zhang, H., 2015. Preparing high surface area porous carbon from biomass by carbonization in a molten salt medium. RSC Adv. 5, 75728–75734. https://doi.org/10.1039/C5RA12406A.

Spierling, S., Knüpffer, E., Behnsen, H., Mudersbach, M., Krieg, H., Springer, S., Albrecht, S., Herrmann, C., Endres, H.-J., 2018. Bio-based plastics - A review of environmental, social and economic impact assessments. Journal of Cleaner Production 185, 476–491. https://doi.org/10.1016/j.jclepro.2018.03.014.

Sutivisedsak, N., Cheng, H.N., Burks, C.S., Johnson, J.A., Siegel, J.P., Civerolo, E.L., Biswas, A., 2012. Use of Nutshells as Fillers in Polymer Composites. J Polym Environ 20, 305–314. https://doi.org/10.1007/s10924-012-0420-y.

Tieke, B., 2014. Makromolekulare Chemie: Eine Einführung. John Wiley & Sons.

Vasanthan, N., Salem, D., 2001. FTIR Spectroscopic Characterization of Structural Changes in Polyamide-6 Fibers during Annealing and Drawing 0488. https://doi.org/10.1002/1099-0488(20010301)39.

Zaaba, N.F., Ismail, H., Jaafar, M., 2013. Effect of peanut shell powder content on the properties of recycled polypropylene (RPP)/peanut shell powder (PSP) composites. BioResources 8, 5826–5841. https://doi.org/10.15376/biores.8.4.5826-5841.

Zhang, Q., Chen, W., Qu, G., Lin, X., Han, D., Yan, X., Zhang, H., 2019. Liquefaction of Peanut Shells with cation exchange resin and sulfuric acid as dual catalyst for the subsequent synthesis of rigid polyurethane foam. Polymers 11, 1–12. https://doi.org/10.3390/polym11060993.

Zierdt, P., Theumer, T., Kulkarni, G., Däumlich, V., Klehm, J., Hirsch, U., Weber, A., 2015. Sustainable wood-plastic composites from bio-based polyamide 11 and chemically modified beech fibers. Sustainable Materials and Technologies 6, 6–14. https://doi.org/10.1016/j.susmat.2015.10.001.